Rogério V. Jacomini[1], Filipe S. Trindade[2], Alfeu J. Sguarezi Filho[1], Ernesto Ruppert[2]

Centro de Engenharia, Modelagem e Ciências Sociais Aplicadas Universidade Federal do ABC Santo André (1),
Faculdade de Engenharia Elétrica e da Computação Universidade Estadual de Campinas (2)

Decoupled Power Control for Doubly-Fed Induction Generator Using Sliding-Mode Control

Abstract. *This paper proposes a decoupled control of active and reactive power for doubly-fed induction generators (DFIG) through the rotor currents using sliding mode control (SMC). In order to decouple the active and reactive power generated, stator-flux-oriented vector control is applied. The sliding mode control strategy proposes is based on two sliding modes plus PI controllers whose main advantage is the easy implementation. Simulation and experimental results are presented to validate the proposed control scheme for a 2 kW DFIG during stator active and reactive power steps and speed variation. During transient operation it is checked good dynamic response.*

Streszczenie. *W artykule opisano sterowanie mocą czynną i bierną w podwójnie zasilanym generatorze indukcyjnym DFIG za pośrednictwem prądu wirnika z wykorzystaniem metody ślizgowej SMC. Zastosowano sterowanie wektora strumienia stojana. Symulacje i badania eksperymentalne potwierdziły założenia możliwości sterowania systemem DGFIG 2 KW przy różnych prędkościach. Badano także właściwości dynamiczne. (Rozsprzężone sterowanie mocą w generatorze DFIG przy wykorzystaniu metody ślizgowej)*

Keywords: Doubly-fed induction generator, DFIG, flux orientation, vector control, power control, sliding mode control
Słowa kluczowe: generator DFIG, sterowanie mocą, sterowanie ślizgowe

List of symbols

R_1, R_2	Stator and rotor resistances.
L_1, L_2	Stator and rotor self inductances.
L_m	Mutual inductance.
ω_1	Synchronous angular speed.
ω_{mec}	Mechanical angular speed.
θ_s, θ_r	Stator flux vector and rotor angles
P, Q	Active and reactive power.
$\overline{v}$	Voltage space vector.
$\overline{i}$	Current space vector.
$\overline{\lambda}$	Flux linkage space vector.

Superscripts

$*$	Reference value

Subscripts

$1, 2$	stator and rotor, respectively
α, β	direct- and quadrature-axis expressed in the stationary reference frame
d, q	direct- and quadrature-axis expressed in the synchronous reference frame
m, n	direct- and quadrature-axis expressed in the rotor reference frame

Introduction

The renewable energy systems have attracted interest due to the increasing concern about the emission of carbon dioxide and other poluent gases. From the many options of renewable sources, one which has obtained and will continue to obtain a great attention is the wind energy.

DFIG based wind turbines have been one of the most emergent technologies for this kind of electric energy generation, since this kind of asynchronous machine is a cost effective, efficient and reliable solution [1]. The typical topology of a DFIG based wind turbine connected to the grid is shown on Fig. 1.

The generator's stator can be connected directly to the grid, from which mostly of the generated power is delivered to the grid. The rotor is conected to a bidirectional converter

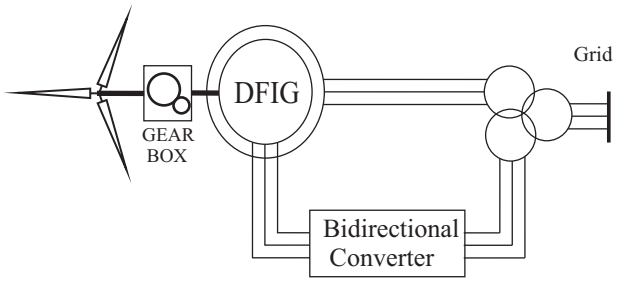

Fig. 1. Configuration of DFIG connected direct on grid with a Sliding Mode Controller.

that is connected to the grid. This converter controls the rotor voltage (thus the generated energy) and the connection with the grid [2].

As in control of induction motor that uses vector control for field orientation for high dynamic performances [3], the vector control is also widely used in control of DFIG. The control of the wind turbine system can be based on either stator-flux-oriented vector control [4] or stator-voltage-oriented vector control [5]. The scheme decouples the rotor current into active and reactive power components and, with a rotor current controller, the power control is achieved. Some investigations using PI controllers that creates rotor current references to the inverter from active and reactive power errors or in-series-PI controllers that results in rotor voltage references have been presented by [4, 6, 7]. PI controllers are also applied to DFIG under grid voltages dips conditions [8, 9]. The problems in using PI controllers are the tunning, the cross-coupling of DFIG terms and it's slow response. To avoid the use of PIs, in [19] proposes controllers for field orientation control (FOC) based on the dynamic modeling of the DFIG, however, is a strategy that presents a high computational cost and only simulation results is presented.

The Sliding Mode Control strategy is a variable structure control method. It is an alternative to the classic control theory for a noncontinuous control implementation [10, 11]. This kind of control has a switching characteristic, which becomes an interesting process when applied to switching power converters [12]. In [14] was proposed a sliding mode approach for direct torque control of sensorless induction motor drives. With regard to the control of DFIG, power reg-

ulation or torque regulation techniques, such as direct torque control (DTC) [13, 14], direct power control(DPC) [15, 16] has been investigated displaying excellent dynamic performance and a cutting-in no-load application for field oriented control (FOC) [17]. However, many of these techniques present variable switching frequency (which complicates the AC filter design), current distortion or they are very dependent on the machine parameters. A nonlinear controller based on sliding mode, described in the stationary coordinate system is implemented by [18], however, the control objective is the operation under voltage sag and the controller design is developed from the dynamic equations of the DFIG, including terms representing the uncertainties and disturbances in the network, making it hard your project.

This paper proposes a new alternative power control scheme for DFIG using sliding mode controllers with stator-flux-oriented vector control. The SMC proposed is based on two sliding modes plus PI controllers, one of its main advantages is the low computational cost for implementation, good response dynamics of power and excellent performance during speed variation. The output of SMC generates the reference values of d- and q-axis rotor voltages, where d-axis is generated by reactive power law and q-axis by the active power control law, where are transformed to the coordinate system fixed on the rotor and used in space vector modulation (SVM). The SMC strategy combined with the SVM has excellent performance in terms of low power ripple. Simulation and experimental results are presented to validate the proposed control scheme.

Machine Model

The doubly-fed induction generator model in the synchronous reference frame was given by [21] and it is described by the following equations:

$$\vec{v}_{1dq} = R_1\vec{i}_{1dq} + \frac{d\vec{\lambda}_{1dq}}{dt} + j\omega_1\vec{\lambda}_{1dq} \tag{1}$$

$$\vec{v}_{2dq} = R_2\vec{i}_{2dq} + \frac{d\vec{\lambda}_{2dq}}{dt} + j\left(\omega_1 - NP\omega_{mec}\right)\vec{\lambda}_{2dq} \tag{2}$$

where the relationship between magnetic fluxes and currents are done by:

$$\vec{\lambda}_{1dq} = L_1\vec{i}_{1dq} + L_M\vec{i}_{2dq} \tag{3}$$

$$\vec{\lambda}_{2dq} = L_M\vec{i}_{1dq} + L_2\vec{i}_{2dq} \tag{4}$$

and generator's active and reactive power are done by:

$$P = \frac{3}{2}\left(v_{1d}i_{1d} + v_{1q}i_{1q}\right) \tag{5}$$

$$Q = \frac{3}{2}\left(v_{1q}i_{1d} - v_{1d}i_{1q}\right) \tag{6}$$

The subscripts 1 and 2 represent, respectively, the stator's and rotor's parameters and variables; ω_1 represents the synchronous speed; ω_{mec} represents the generator's mechanical speed; R_1 and R_2 represent the stator's and the rotor's per phase electrical resistance; L_1, L_2 and L_m represent the stator's and the rotor's windings proper and mutual inductances; $\vec{v}$, $\vec{i}$ and $\vec{\lambda}$ represent, respectively, the voltage, the current and the flux space vector; and NP represents the machine's number of pole pairs.

The proposed power control aims independent stator active P and reactive Q power control by means of a rotor current regulation. For this purpose, P and Q are represented as functions of each individual rotor current. To achieve this objective, the stator-flux-oriented vector control method decouples the dq axis and makes $\lambda_{1d} = \lambda_1 = |\vec{\lambda}_{1dq}|$. Thus, (3) becomes

$$i_{1d} = \frac{\lambda_1}{L_1} - \frac{L_M}{L_1}i_{2d} \tag{7}$$

$$i_{1q} = -\frac{L_M}{L_1}i_{2q} \tag{8}$$

Similarly, the stator voltage becomes $\vec{v}_{1d} = 0$ and $v_{1q} = v_1 = |\vec{v}_{1dq}|$. Hence, the active (5) and reactive (6) powers can be calculed by using the Equations (7) and (8)

$$P = -\frac{3}{2}v_1\frac{L_M}{L_1}i_{2q} \tag{9}$$

$$Q = \frac{3}{2}v_1\left(\frac{\lambda_1}{L_1} - \frac{L_M}{L_1}i_{2d}\right) \tag{10}$$

The stator current can be computed by using the rotor current. Consequently, this principle can be used on stator's active and reactive power control by controlling the currents in the rotor side with the generator's stator terminals connected directly to the grid.

SMC applied to the DFIG power control

The essential idea of traditional VSC control algorithms is to enforce the system mode to slide along a predefined sliding surface of the system state space [10]. Once the state of the system reaches the sliding surface, the structure of the controller is adaptively changed to slide the state of the system along the sliding surface. Hence, the system response depends only on the predefined sliding surface and remains insensitive to variations of system parameters and external disturbances. However, such insensitivity property is not guaranteed before sliding mode occurs, resulting in the loss of the robustness during the reaching phase. Furthermore, in order to reduce the chattering, the sign function of VSC is often replaced by saturation function in practical implementations [20].

The proposed strategy uses the sliding mode controller and the stator-flux-oriented control to regulate the rotor currents and the active and reactive power based on (9) and (10).

It's defined the error between the current references and the measured values to obtain the sliding surface as

$$e_{i2d} = i_{2dref} - i_{2d} \tag{11}$$

$$e_{i2q} = i_{2qref} - i_{2q} \tag{12}$$

where i_{2d} and i_{2q} are the rotor currents calculated on the dq referential frame. i_{2dref} and i_{2qref} are the rotor current

references in the dq reference frame given by

$$i_{2qref} = -\frac{2P_{ref}L_1}{3v_1L_M} \tag{13}$$

$$i_{2dref} = -\frac{2Q_{ref}L_1}{3v_1L_M} + \frac{\lambda_1}{L_M} \tag{14}$$

The sliding surface S can be defined as

$$S = \begin{bmatrix} s_1 \\ s_2 \end{bmatrix} = \begin{bmatrix} e_{i2d} + c_{i2d}\frac{d}{dt}(e_{i2d}) \\ e_{i2q} + c_{i2q}\frac{d}{dt}(e_{i2q}) \end{bmatrix} \tag{15}$$

where c_{i2d} and c_{i2q} are constants defined taking into account the desirable dynamic response for the system.
According to the Equations (13) and (14), the rotor current d component is responsible for the reactive power control and, the rotor current q component, is responsible for the active power control. This way, the control objective is to make the system state go to the equilibrium point defined on the origin of the sliding surface ($S = 0$), where the errors and their derivatives are zero, ensuring that the states reach their references.
Based on [14], for active and reactive power control by regulating rotor currents, the rotor voltage references are given by

$$v_{2dref} = \left(K_{Pi2d} + \frac{K_{Ii2d}}{s}\right).eval(s_1) \tag{16}$$

$$v_{2qref} = \left(K_{Pi2q} + \frac{K_{Ii2q}}{s}\right).eval(s_2) \tag{17}$$

where K_{Pi2d} and K_{Pi2q} are the proportional gains and K_{Ii2d} and K_{Ii2q} are the integral gains as for a PI controller; v_{2dref} and v_{2qref} are rotor voltage references on dq reference frame; and, $eval(s_1)$ and $eval(s_2)$ are evaluation functions that determine the switching behavior of the controller once the responses reach the sliding surface.
The $eval$ function can be simple as the signal function. However in this case, it was used a saturated linear function, as given by

$$eval(s_n) = \begin{cases} max, & \text{if} \quad K.s_n \geq max, \\ K.s_n, & \text{if} \quad min < K.s_n < max, \\ min, & \text{if} \quad K.s_n \leq min. \end{cases} \tag{18}$$

where n can be 1 or 2, depending on the sliding surface of the Eq. (15) is used.

– Description of the implemented control system

The block diagram of the proposed control scheme is shown in Fig. 2 and in Fig. 3 is shown the details of the SMC block.

The desired rotor voltage in the rotor mn reference frame generates pulse width modulation (PWM) switching signals for the rotor side using either space vector modulation (*SVM*) that is given by $v^*_{2,mn} = v^*_{2,dq}\, e^{\theta_s - \theta_r}$. The stator currents and voltages, rotor speed and currents are measured to stator flux position θ_s and magnitude λ_s and synchronous frequency ω_1 estimation.

The flux estimation is obtained using the following equation

$$\vec{\lambda}_{1,\alpha\beta} = \int \left(\vec{v}_{1,\alpha\beta} - R_1\vec{i}_{1,\alpha\beta}\right) dt \tag{19}$$

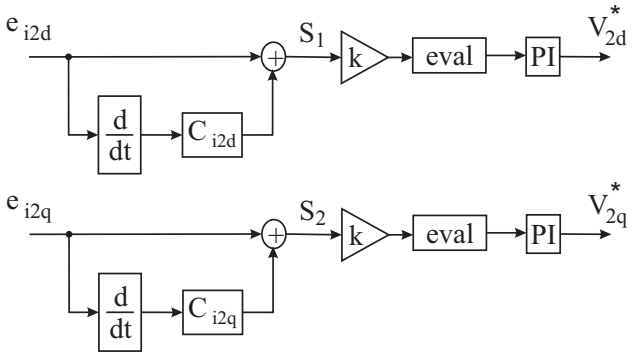

Fig. 2. Configuration of DFIG connected direct on grid with a Sliding Mode Controller.

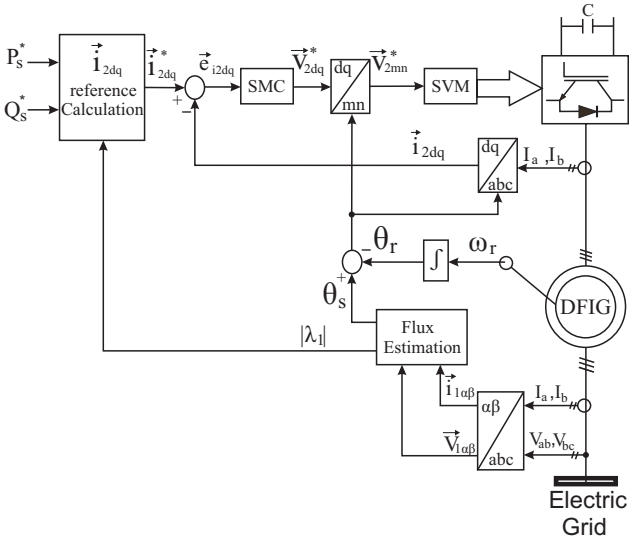

Fig. 3. The Sliding Mode Controller for DIFG power control.

and the flux position by using (19) as

$$\theta_s = \arctan\left(\frac{\lambda_{1\beta}}{\lambda_{1\alpha}}\right) \tag{20}$$

The synchronous speed ω_1 estimation is given by

$$\omega_1 = \frac{d\theta_1}{dt} = \frac{(v_{1\beta} - R_1 i_{1\beta})\,\lambda_{1\alpha} - (v_{1\alpha} - R_1 i_{1\alpha})\,\lambda_{1\beta}}{(\lambda_{1\alpha})^2 + (\lambda_{1\beta})^2} \tag{21}$$

To maintain the *SVM* in the linear zone of operation, the rotor voltage $\overline{v}^*_{2,mn}(k)$ is limited as follows

$$|\overline{v}^*_{2,mn}(k)| = \sqrt{v^{*2}_{2m}(k) + v^{*2}_{2n}(k)} \tag{22}$$

$$\theta(k) = \arctan\frac{v^*_{2n}(k)}{v^*_{2m}(k)} \tag{23}$$

$$\text{if} \quad |\overline{v}^*_{2,mn}(k)| >= v_{2,max} \quad \text{then} \quad |\overline{v}^*_{2,mn}(k)| = v_{2,max}$$

$$v^*_{2m}(k) = |\overline{v}^*_{2,mn}(k)|\cos[\theta(k)] \tag{24}$$

$$v^*_{2n}(k) = |\overline{v}^*_{2,mn}(k)|\sin[\theta(k)] \tag{25}$$

where $v_{2,max}$ is the maximum rotor phase voltage that the converter can produce. So for the power electronic converter provides the maximum voltage ($v_{2,max}$) is necessary a voltage dc link given by

$$V_{DC} = \frac{\sqrt{3} \times v_{2,max}}{(N_s/N_r) \times m} \tag{26}$$

where *m*=1.25 is the modulation index of SVM and (N_s/N_r) is the stator/rotor turns ratio of the DFIG.

Simulation and Experimental Results

The SMC strategy proposed has been simulated using the Simulink on a 2.2 kW DFIG, whose nominal values are given in Appendix. To validate the simulation results, the SMC strategy is also applied to a DSP TMS320F2812 platform. The rotor windings are fed by a three-phase voltage source inverter with with insulated-gate bipolar transistors (IGBTs) and the DFIG is driven by a DC motor. The rotor voltage commands are modulated by using symmetrical space vector PWM, with switching frequency equal to 5 kHz. The DC bus voltage of the inverter is 120 V. The encoder resolution is 3800 pulses per revolution. The experimental setup is shown in Fig. 4. System parameters, including control loop parameters, that were obtained from simulation tests, are shown in Appendix.

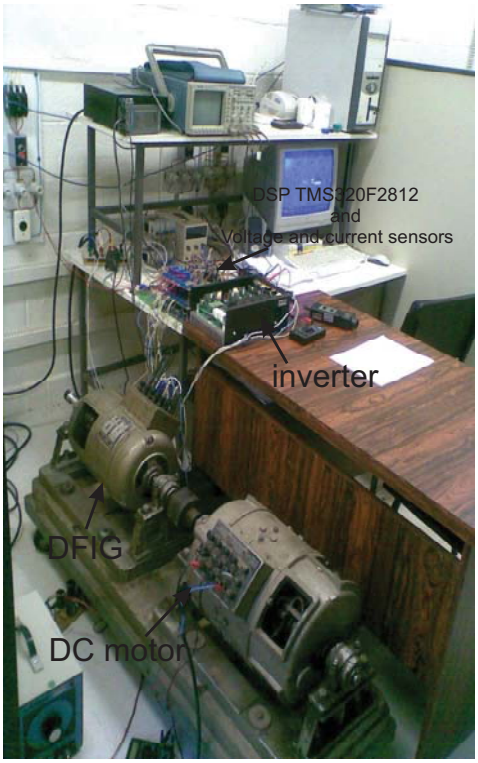

Fig. 4. Experimental setup for power control implementation.

– Constant Speed Operation

Firstly, the generator is operating in the subsynchronous mode, driven in a constant speed of 1350 rpm (75% of the machine's synchronous speed) and it was tested with various active and reactive power steps as set points to test the dynamic response of the control strategy, as shown in Fig. 5(a). The initial active power and the power factor references were, respectively, -2kW and +1. The active power and the power factor references were changed from -2kW to -1kW and from +1 to -0.85 (capacitive) at $400ms$, respectively. Finally, at $700ms$, the active power reference was changed from -1kW to -1.5kW and, the power factor, from -0.85 to +0.85 (inductive). One observes that during the changes power references, which are the controlled variables, the SMC strategy generates the required control voltage (v_{2d}^* and v_{2q}^*) from the errors between the references and actual values of the d-q rotor current components, resulting in a transient responses within a few milliseconds of both powers of mode decoupled without overshoot and zero error regime. Fig. 6 shows the transitory of stator power in detail when the active power and the power factor references changed from -2kW to -1kW and from +1 to -0.85 (capacitive), respectively, which demonstrates the good performance of the proposed controller. The d-q components of the rotor current for this test is shown in Fig. 5(b), verifying that the values measured of the d-q rotor current components are quickly following their respective reference values calculated for the control of active and reactive power. The rotor current in $\alpha\beta_r$ and the phase a stator current and voltage during this test are shown in Figs. 5(c) and 7, respectively.

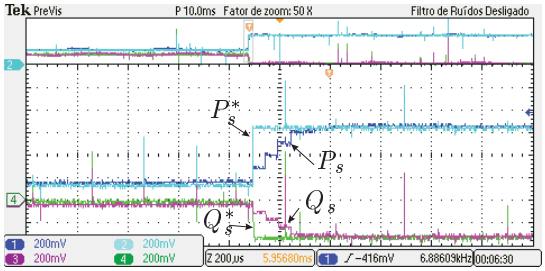

Fig. 6. Zoom of the step response for active power and the power factor references changed from -2kW to -1kW and from +1 to -0.85 (capacitive), respectively.

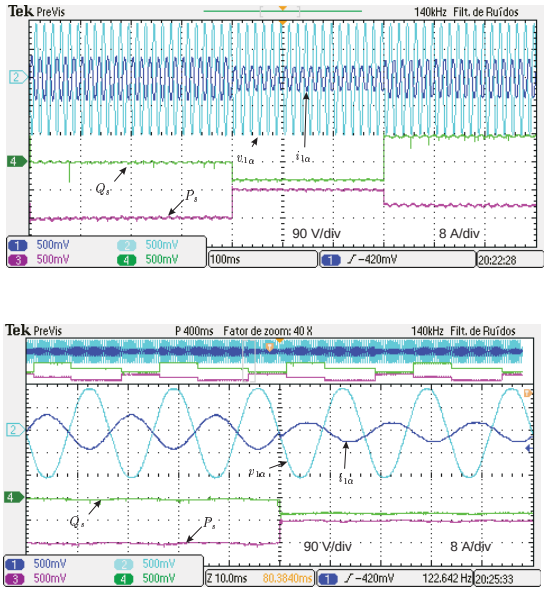

Fig. 7. Stator voltage and current during the step response in fixed speed operation.

– Variable Speed Operation

During this test, the generator was driven with a speed profile that varies from 1600 rpm (subsynchronous) to 1975 rpm (supersynchronous) and it was tested with various active and reactive power steps (Fig. 8(a)) as performed in previous test. One verifies that even in variable speed operation the controller is able to act to give a quick response of active and reactive power of mode decoupled without overshoot and null steady state error, similarly to the previous test. The d-q components of the rotor current during this test are shown in Fig. 8(b). In Fig. 8(c) shows the waveform of the rotor current in $\alpha\beta_r$ during the rotor speed variation.

Conclusion

This paper proposed a SMC applied to the DFIG power control. The rotor voltage is calculed by SMC controller by using slides surfaces based on the rotor current errors, eval functions and PI controllers. Hence, this control technique

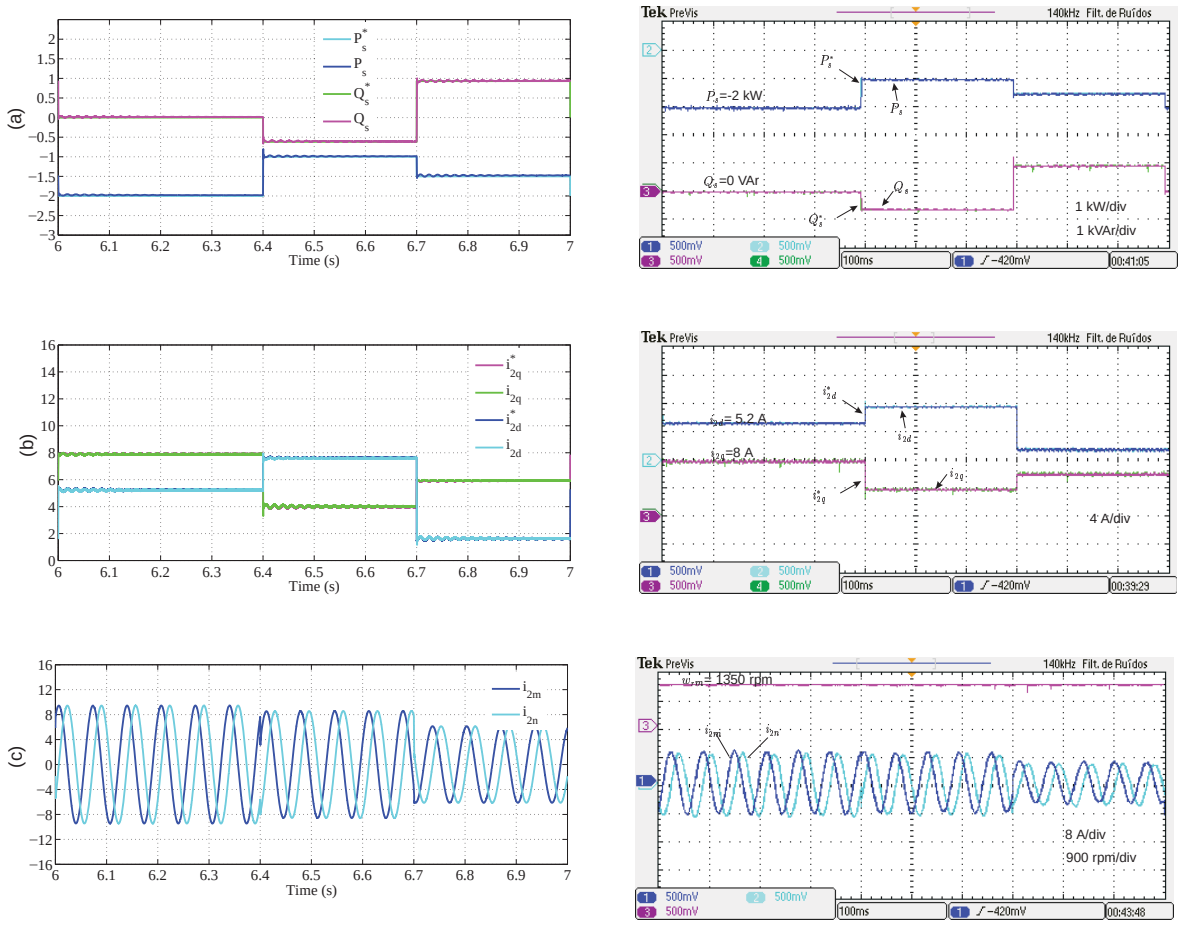

Fig. 5. Simulation and experimental results during tested with various active and reactive power steps in fixed speed operation. (a) Active and reactive power [kW and kVAr]. (b) Synchronous d-q axis rotor current [A]. (c) Rotor α_r-β_r axis rotor current and rotor speed [A and rpm].

allows that the power and rotor current fallow the references. Simulation and experimental results have shown satisfactory performance – fast dynamic response – with respect to several step response tests, both at constant and variable rotor speeds. The SMC during these tests has resulted in good responses, with minor steady state error and overshoot. Hence, it was concluded that the SMC strategy can be an interesting tool for the power control of the DFIG.

Appendix

Doubly-fed induction generator parameters:

$R_1 = 1.2\ \Omega$; $R_2 = 0.8\ \Omega$; $L_m = 0.092\ H$; $L_{l1} = 0.00618\ H$; $L_{l2} = 0.00618H$; $NP = 2$; $P_N = 2.2\ KW$; $V_N = 220\,V$.

Controllers' parameters:

Table 1. Controllers' constants and parameters.

Specification	SMC$_d$	SMC$_q$	PI$_d$	PI$_q$
K_P	5	10	25	25
K_I	10	10	15	15
c_{sn}	10^{-8}	10^{-5}	–	–
K	3	3	–	–
max	50	50	–	–
min	-50	-50	–	–

Acknowledgements

The authors would like to thank CAPES, FAPESP and CNPq for the financial support of this and others researches that are being developed in the LEPO/FEEC/Unicamp.

REFERENCES

[1] Abad, G. and López, J. and Rodríguez, M. and Marroyo, L. and Rodríguez, M. and Iwanski, G., *"Doubly Fed Induction Machine: Modeling and Control for Wind Energy Generation Applications"*, John Wiley & Sons, 2011, pp. 414-421.

[2] Jamal A. Baroudi and Venkata Dinavahi and Andrew M. Knight, *"A review of power converter topologies for wind generators"*, Renewable Energy, Vol. 32, 2007, pp. 2369-2385.

[3] Netto, A.J. and Barros, P.R. and Jacobina, C.B. and Lima, A.M.N. and da Silva, E.R.C., *"Indirect field-oriented control of an induction motor by using closed-loop identification"*, Industry Applications Conference, 2005. Fourtieth IAS Annual Meeting. Oct. 2005, 1357 - 1362 Vol. 2.

[4] Tapia, A. and Tapia, G. and Ostolaza, J.X. and Saenz, J.R., *"Modeling and control of a wind turbine driven doubly fed induction generator"*, IEEE Transactions on Energy Conversion, Vol. 18, N0. 2, Jun. 2003, pp. 194-204.

[5] Baike Shen and Boon-Teck Ooi, *"Novel Sensorless Decoupled P-Q Control of Doubly-Fed Induction Generator(DFIG) Based on Phase Locking to Gamma-Delta Frame"*, Power Electronics Specialists Conference, 2005. PESC '05. IEEE 36th, Jun. 2005, pp. 2670 -2675.

[6] Bradul H. Chowdhury and Srinivas Chellapilla, *"Double-fed induction generation control for variable speed wind power generation"*, Electric Power System Research, N0. 76, 2006, pp. 786-800.

[7] R. V. Jacomini, A. França, E. Bim. *"Simulation and Experimental Studies on Double-fed Induction Generator Power Control Operating at Subsynchronous Operation Speed"*, The Eighth International Conference on Power Electronics and Drive Systems, November 2-5, 2009, Taipei, Taiwan, R.O.C.

[8] Francisco K. A. Lima, Alvaro Luna, Pedro Rodriguez, Edson H. Watanabe and Frede Blaabjerg, *"Rotor Voltage Dynamics in the Doubly Fed Induction Generator During Grid Faults"*, IEEE Trans. on Power Electronics, Vol. 25, N0. 1, Jan. 2010, pp. 118-130.

[9] V. Flores Mendes and C.V. de Sousa and S. Rocha Silva and

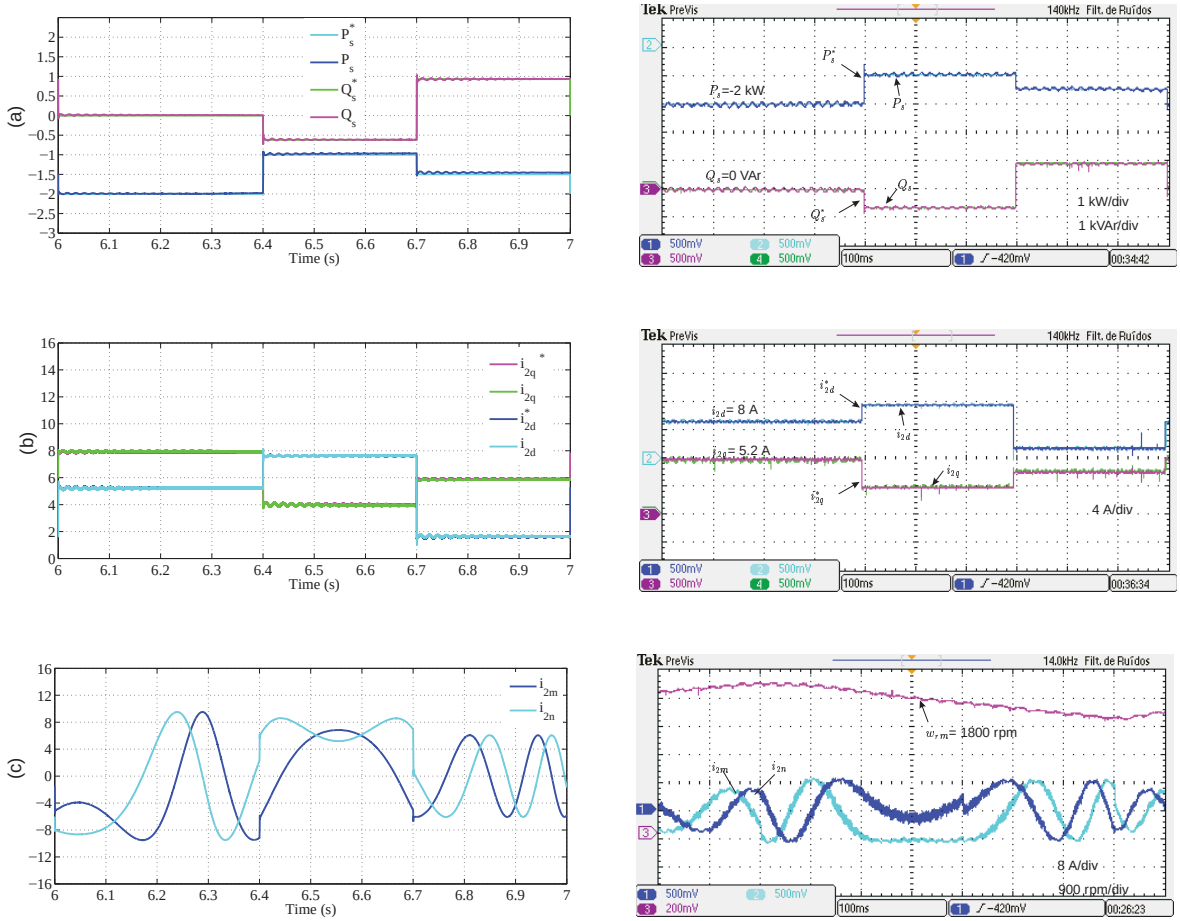

Fig. 8. Simulation and experimental results during tested with various active and reactive power steps in variable speed operation. (a) Active and reactive power [kW and kVAr]. (b) Synchronous d-q axis rotor current [A]. (c) Rotor $\alpha_r - \beta_r$ axis rotor current and rotor speed [A and rpm].

B. Cezar Rabelo and W. Hofmann, *"Modeling and Ride-Through Control of Doubly Fed Induction Generators During Symmetrical Voltage Sags"*, IEEE Transactions on Energy Conversion, Vol. 26, N0. 4, Dec. 2011, pp. 1161 -1171.

[10] Edwards, C. and Spurgeon, S.K., *"Sliding Mode Control: Theory And Applications"*, Taylor & Francis systems and control book series, 1998.

[11] NAOUAR, W. and Monmasson, E. and Naassani, A. and Slama-Belkhodja, I., *"FPGA-Based Dynamic Reconfiguration of Sliding Mode Current Controllers for Synchronous Machines"*, IEEE Transactions on Industrial Informatics, Vol. PP, N0. 99, 2012.

[12] Muhammad Rashid,*"Power electronics circuits, devices and aplications"*,Pretince Hall, 2004.

[13] Chen, S.Z. and Cheung, N.C. and Wong, K.C. and Wu, J., *"Integral variable structure direct torque control of doubly fed induction generator"*, Renewable Power Generation, IET, Vol. 5, N0. 1, Jan. 2011, pp. 18 -25.

[14] Lascu, C. and Boldea, I. and Blaabjerg, F., *"Direct torque control of sensorless induction motor drives: a sliding-mode approach"*, IEEE Transactions on Industry Applications, Vol. 40, N0. 2, march-april 2004, pp. 582-590.

[15] Jiabing Hu and Heng Nian and Bin Hu and Yikang He and Zhu, Z.Q., *"Direct Active and Reactive Power Regulation of DFIG Using Sliding-Mode Control Approach"*, IEEE Transactions on Energy Conversion, Vol. 25, N0. 4, Dec. 2010, pp. 1028-1039.

[16] Hea Gwang Jeong and Won Sang Kim and Kyo Beum Lee and Byung Chang Jeong and Seung Ho Song, *"A sliding-mode approach to control the active and reactive powers for A DFIG in wind turbines"*, IPower Electronics Specialists Conference, 2008. PESC 2008. IEEE, june 2008, pp. 120-125.

[17] Xuemei Zheng and Wei Li and Wei Wang, *"High-order sliding mode controller for no-load cutting-in control in DFIG wind power system"*, Systems and Control in Aeronautics and Astronautics (ISSCAA), 2010 3rd International Symposium on, june 2010, pp. 1304 -1308.

[18] J. P. da Costa and H. Pinheiro and T. Degner and G. Arnold, *"Robust Controller for DFIGs of Grid-Connected Wind Turbines"*, IEEE Transactions on Industrial Eletronics, Vol. 58, N0. 9, Set. 2011, pp. 4023-4038.

[19] A. J. Sguarezi Filho and M. E. de oliveira Filho and E. Ruppert, *"A predictive power control for wind energy"*, IEEE Transactions on Sustainable Energy, Vol. 2, 2011, pp. 97-105.

[20] M. V. Lazarini and E. Ruppert Filho, *"Induction motor control didactic set-up using sensorless and sliding mode dtc strategy"*, Eletrônica de Potência, Vol. 13, N0. 4, 2008, pp. 291-299.

[21] W. Leonhard, *"Control of Electrical Drives"*, Springer-Verlag Berlin Heidelberg New York Tokyo, 1985.

Authors:

Ph.D. Rogério V. Jacomini, M. Sc. Filipe S. Trindade**, Prof. Ph.D. Alfeu J. Sguarezi Filho*, Prof. Ph.D. Ernesto Ruppert**,*

**Centro de Engenharia, Modelagem e Ciências Sociais Aplicadas da Universidade Federal do ABC - UFABC - Santo André Brasil,*

***School of Electrical and Computer Engineering of State of Campinas - UNICAMP - Campinas Brazil,*

email: rogeriojacomini@gmail.com, alfeu.sguarezi@ufabc.edu.br, ruppert@fee.unicamp.br.